Applied Journal of Environmental Engineering Science

Kinetic and Thermodynamic evaluation on Removal of Anionic Dye from Aqueous Solution using Activated Carbon Derived from Agricultural Waste: Equilibrium and Reusability Studies

***Musa Husaini, Bishir Usman and Muhammad Bashir Ibrahim**

Department of Pure and Industrial Chemistry, Faculty of Physical Sciences College of Natural and Pharmaceutical Sciences, Bayero University Kano (BUK), P.M.B. 3011, Kano, Nigeria.

Corresponding author. E-mail address: mbibrahim.chm@buk.edu.ng
Received 07 Jun 2023, Revised 30 Jul 2023, Accepted 16 Sep 2023

Abstract

Nowadays, the presence of dye in aqueous solutions is a major environmental concern. Activated carbon of ginger bread plum (GBPA) was studied as agricultural wastes derived adsorbent for the removal of methyl orange (MO) from aqueous solutions using batch adsorption technique. The adsorbent was characterized using point of zero charge (PZC), Scanning Electron microscopy (SEM) and Fourier Transform Infra-Red (FTIR) spectroscopy. Batch adsorption experiments were conducted to elucidate the impact of experimental parameters such contact time (5 – 150 minutes), adsorbent dosage (0.1 – 0.6g), particle size (75 - 900 µm), initial dye concentration (20 – 500 mg/L), pH (2 -12) and temperature (303 – 323 K). Pseudo-first order and pseudo-second order were used to described the kinetic behavior of the process and the data from the experimental result accord with pseudo second order with $R^2 = 0.9999$. The equilibrium data was also computed using Langmuir, Temkin, Freundlich, and D-R models and was found to follow Freundlich adsorption isotherm. Thermodynamics studied parameters such as change in enthalpy (ΔH), entropy (ΔS) and Gibbs free energy of adsorption (ΔG) clearly indicates that the adsorption process was feasible endothermic and spontaneous in nature. Desorption was performed using various eluent and reusability of the adsorbent was done in five successive cycles.

Key words: *Adsorption, Desorption, Kinetics, Methyl orange, Reusability, Thermodynamic.*

1. Introduction

The water quality was significantly affected by the climate change, industrial development and rapid growth of the global population leading to an increasing freshwater crisis globally [1]. Consequently, freshwater depletion was contributed significantly by numerous consumers and polluters [2]. Out of them, increasingly used dye such as methyl orange and others are the most usual industrial pollutant sources that originate from various industries like cosmetic, textile, food, leather, pulp and paper industries, paint and varnish and

pharmaceutical industries [3 and 4]. Almost 70 tons of dyes are annually produced worldwide according to the recent research [5].

Environment and human health are jeopardizes by the presence of this industrial waste dye into water bodies. The photosynthetic process in aquatic ecosystems might be adversely affected by upon direct release of non-treated effluent into natural water source [6]. It causes teratogenic and mutagenic effect on fish species and other aquatic organisms due to the presence of metals and aromatics [7]. Additionally, the existence of dyes in the environment lead to serious toxic effect to human health, consisting kidney disease, dermatitis effects, allergic mutagenic and carcinogenic [8]. Thus, human health, aquatic life and water bodies can be affected by the disposal of dyes into the environment. The remediation of dye wastewater using different methods such as filtration, advanced oxidation, ion-exchange, electrocoagulation, adsorption, coagulation, constructed wetlands, moving bed biofilm [9]. Adsorption become one of the most useful decontamination process. It is considered to be a sludge free process, low cost, fast, having high mechanical stability, selectivity, recycling facilities and is widely used for the removal of various pollutants from wastewater, including dyes and heavy metals [10 and 11].

Numerous adsorbent, such as polymer-based materials, metal–organic framework, bio-adsorbent, carbon-based, oxide-based and activated carbon has been applied for the adsorption of dyes from wastewater [12]. These adsorbents possess the advantage of large number of active sites, high reactivity, high surface volume ratio, multi-functionalities, high effective surface area, easy fabrication, low cost, reusability and good efficiency to treat recalcitrant compounds [13].

In this research, activated carbon derived from sweet detar was utilized to remove methylene blue dye from aqueous solution. The effect of experimental parameters on the efficiency and adsorption capacity were investigated using batch experimental methods. Kinetics and thermodynamic parameters for the adsorption of methyl orange onto GBAC was studied together with isotherm models to propose the adsorption mechanism for the process.

2. Materials and methods

a. Material

All the reagents used in this research were of analytical and used further purification. Preparation of stock and other working solutions were done by double distilled water. Methyl orange dye was obtained from BDH Chemical, England. The chemical structure of the used dye is presented in figure 1. Sweet detar seed shell was obtained, treated and used as the adsorbent.

b. Sample Collection and Activated Carbon Preparation

Samples of *sweet detar* were collected from a market Katsina Local Government area of Katsina State, Nigeria. Shells were separated from the seeds, washed to remove any dirty material and allowed to sundry for 72 hours. Granular mess was used to grind the sample and impregnated with (30%) phosphoric acid solution for 24 hours and dried prior to carbonization. The sample was then carbonized for 2 hours at 400^0 C using muffle furnace. It was then washed with distilled water to neutral solution and then oven dried at

105^0 C until constant weight [14]. The sweet dater activated carbon sample (GBAC) was then sieved and sealed in an air-tight container.

c. Preparation of Dye Solution

According to the standard method of preparation, 1.0g of methyl orange was dissolved in 1000 cm^3 of distilled water to prepare 1000 mg/L of the stock solution. The smaller experimental solutions of different concentrations (20 – 500 mg/L) were prepared by serial dilution with distilled water. The maximum absorption of the dye was obtained at 464.5 nm using Model Hitachi 2800 UV–Visible spectrophotometer [15].

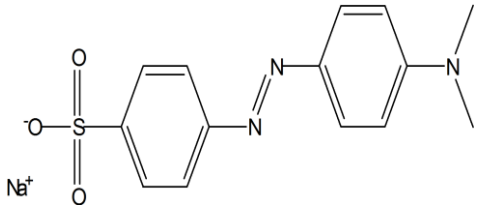

Fig. 1: Structure of Methyl orange

d. Adsorbent Characterization

Fourier 133 Transform Infrared Spectrophotometer was used to analyzed the possible functional of the adsorbent before and after the adsorption process. The sample was analyzed at 32 scans at 8 cm-1 resolution by scanning through a wave number of 650 – 4000 cm^{-1} range. However the surface morphological properties of the adsorbent were also characterized by using scanning electron microscopic analysis before and after the adsorption process. The micrographs from Phenom World Eindhoven Electron Microscope were taken at magnification of x1000 through an accelerating voltage of 15 kV [16].

e. Determination of pH at Point of Zero Charge (pHpzc)

The pH of 0.1 M $NaNO_3$ was adjusted using 0.50 M HCl and NaOH to a desired value between 2 and 10. The mass of the adsorbent (0.1 g) was added to the volume (50 ml) of the adjusted solution in a different conical flask followed by shaking for a period of 24hours. The final pH was recorded, difference between initial and final pH was plotted and the point of intersect the pH line was recorded as the point of zero charge [17].

f. Batch Adsorption Experiments

Batch adsorption process was conducted to obtained the optimum condition for adsorption equilibrium of methyl orange dye onto the surface of GBAC. Various experimental parameters such as contact time, particle size, initial dye concentration, adsorbent dosage, pH and temperature were studied. One parameter varied and all other parameters kept constant for the optimization of the process. The experiments involve running the system in 100ml conical flask containing 0.1 g of adsorbent and 50ml of dye solution inside the mechanical shaker for a desired equilibrium time. The conical flask flask was then removed the content

was filtered using whatman filter paper and the filtrate was analyzed spectrometrically at maximum absorbance wavelength [18-19].

The percentage of dye removal and the mount of dye adsorbed per unit mass of the adsorbent were calculated by using equation 1 and 2 respectively;

$$R\ (\%) = \frac{C_0 - C_e}{C_0} \times 100 \quad (1)$$

Equilibrium adsorption capacity qe of the dye was be calculated by equation 3.

$$qe = \frac{(C_0 - C_e) \times v}{m} \quad (2)$$

Where C_0 (mg/L) and C_e (mg/L) are dye concentration initially and at a given time, V is the volume (L) of the dye solution and m is the mass (g) of the adsorbent.

g. Desorption and Reusability Studies

Various eluent were used to study the desorption of methyl orange loaded adsorbent including sodium chloride (NaCl), distilled water (H_2O), hydrochloric acid (HCl) and sodium hydroxide (NaOH). Distilled water was used to wash the spent adsorbent to remove any trace of unadsorbed dye and later allowed to dry. 0.1 g of the dye loaded adsorbent was added to a set of flasks containing 50ml of eluent and agitated at 200 rpm for 90 minutes. The eluent with higher desorption efficiency was taken for the test of other parameters. The adsorbent was reused in a number of 5 consecutive cycles [20]. Equation 3 and 4 were to evaluate desorption efficiency and desorption capacity.

$$\text{Desorption efficiency } (\%) = \frac{q_{de}}{q_{ad}} \times 100 \quad (3)$$

$$\text{Desorption capacity } (q_{des}) = \frac{C_{des} \cdot V_{des}}{m} \quad (4)$$

Where C_{des} is dye desorbed concentration (mg/dm^3), V_{des} is the volume of desorbing solution (dm^3), m is the mass of the pre-adsorbed adsorbent (g) and q_{ad} is the quantity adsorbed per unit mass of adsorbent (mg/g).

3. Result and Discussion

a. Characterization of the Adsorbent

The result presented in Fig. 2 and 3 shows the surface functionalities of the activated carbon before and after the adsorption process. The presence of various functional groups obtained before the adsorption changes appreciably by little value after methyl orange adsorption on GBAC surface as illustrated in Table 1. The little shift obtained before and the adsorption might be considered as confirmation of certain interaction between the adsorbent surface and dye molecule [21]. The surface texture and porosity of the adsorbent surface was examined by scanning electron microscopic analysis. Fig. 4 (i and ii) depicted the porous and irregular structure of GBAC. However after MO adsorption the visual porous surface was diminished which confirmed the dye molecule accommodation in the adsorbent pores.

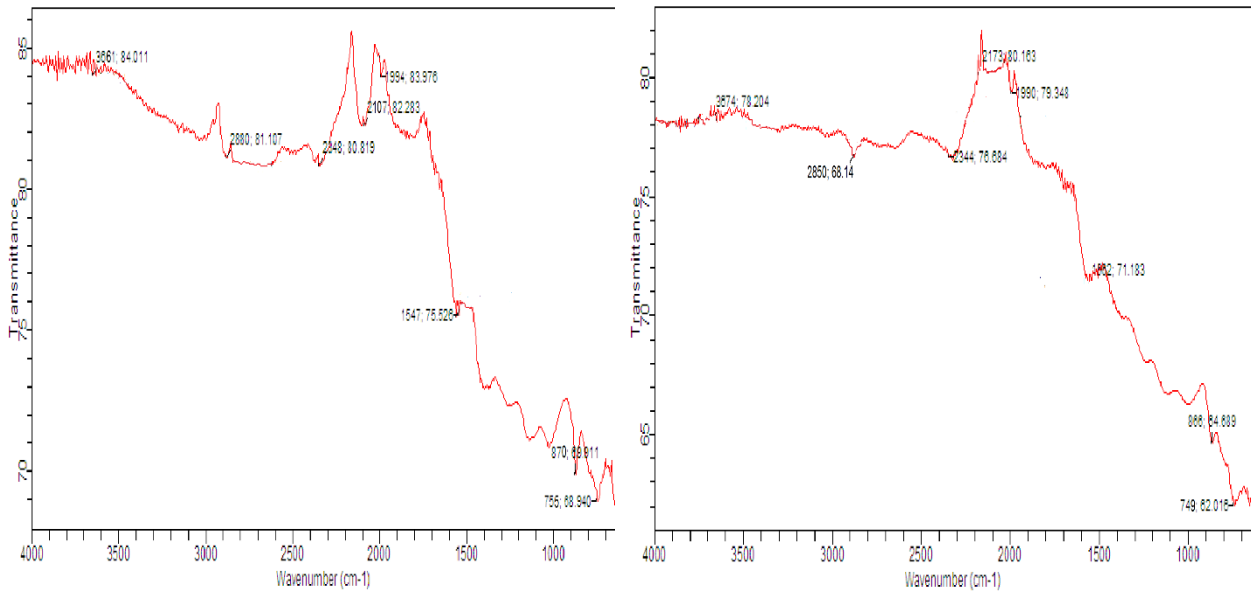

Fig. 2: FTIR Spectra of GBAC i) before and ii) after adsorption

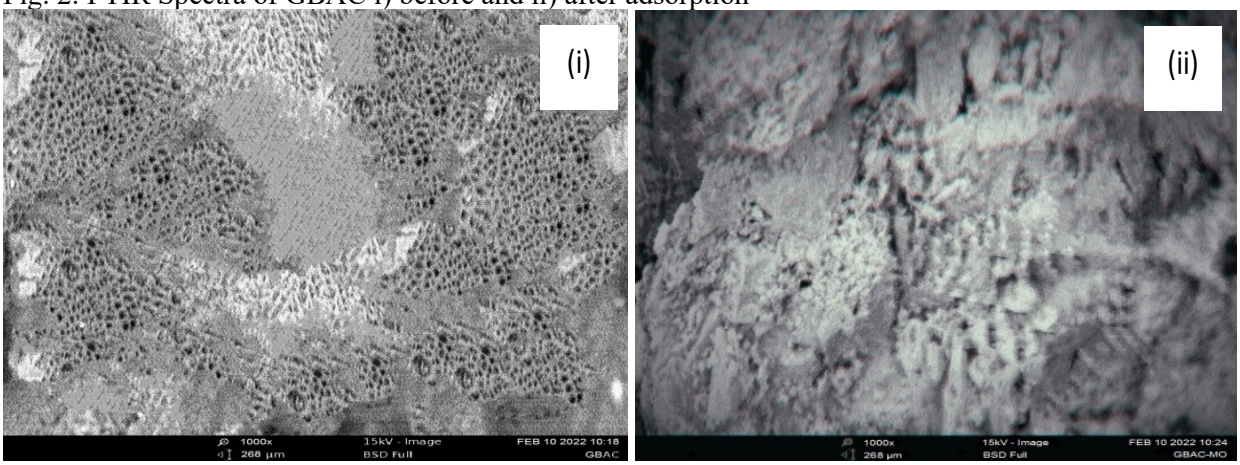

Figures 4: SEM Micrograph (i) GBAC before the adsorption (ii) GBAC -MO after the adsorption

Table 1: Functional group observed before and after adsorption of MO onto GBAC

Functional group	Wavelength range (cm^{-1})	Before Adsorption	After adsorption
O-H stretching vibration in alcohol	3700-3584	3661	3674
C-H stretching vibration in alkane	3000-2840	2880	2850
C ≡ C stretching vibration in alkyne	2260-2100	2191	2258
C ≡ C stretching vibration in alkyne	2260-2190	2107	2173
C=C=C stretching of allene	2000-1900	1988	1990
N-O stretching of nitro groups	1550-1500	1566	1562
C-O stretching of alcoholic groups	1124-1087	1150	1165
C-H bending of 1,3-disubstituted	880±20	898	866
C-H bending of monosubstituted	750±20	743	749

b. Point of Zero Charge (PZC)

The influence of pH on the adsorption can be described based on pH at point of zero charge; it's defined as the point at which the net surface charge of adsorbent functional groups equals to zero under certain condition of pressure and temperature. The pH_{pzc} of the adsorbent is 5.60 as presented in Fig. 5 which falls on a perfect balance charge in the acidic region. Though, acidic water donates H+ in excess than OH- groups and since the adsorbent surface has positive charge on its surface it can therefore favors the adsorption of anionic dye such as MO due to increased electrostatic force of attraction.

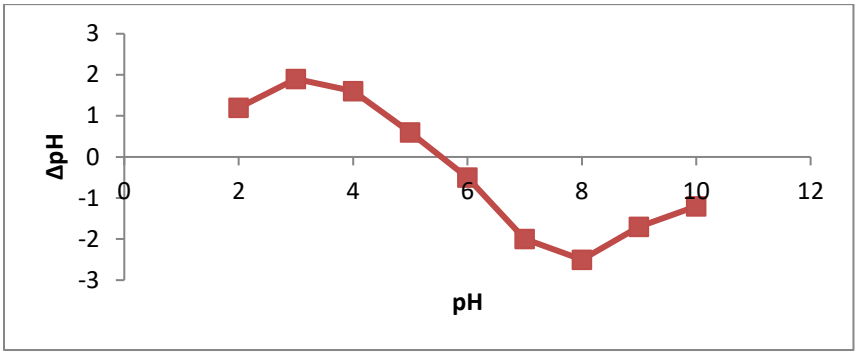

Fig.5: pH at Point of Zero Charge of GBAC

c. Impact of contact time

Adsorption process is time dependent; therefore it's important to investigate the design process in the sorption rate. The effect of contact time for MO with GBAC was studied to obtain the equilibrium time that gave the maximum removal of dye molecules. Fig. 6 shows an increase of adsorption capacity with increase in contact time. At the first stage, initial adsorption was rapid and later keeps on lower rate until it reached equilibrium at 60 minutes which was adopted as the equilibrium time for the testing of the experimental parameters. Therefore, extending the contact time above 60 minutes results to decrease in the adsorption capacity due to the desorption of the adsorbed dye molecules on the adsorbent surface.

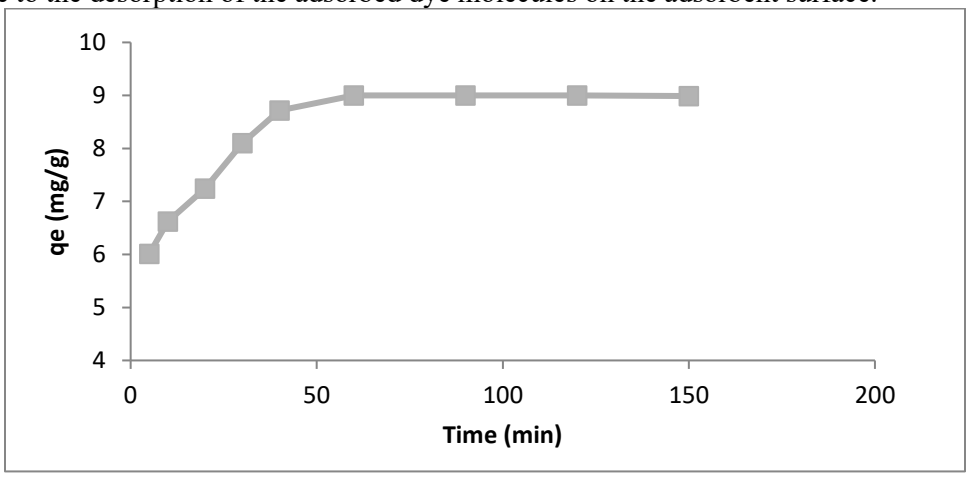

Fig.6: Variation of q_e with Agitation Time

d. Impact of Adsorbent Dosage

The quantity of adsorbent applied in the adsorption process is important as it control the ratio of adsorbate-adsorbent interaction in the process so also in projection cost [22]. The variation of the adsorption capacity adsorbed with adsorbent quantity is presented in Fig. 7. The results show the decrease in adsorption capacity with increase in adsorbent quantity. The decrease in adsorption with an increase in adsorbent weight might be due to partially attributed to the saturation, aggregation or overlapping of adsorption sites.

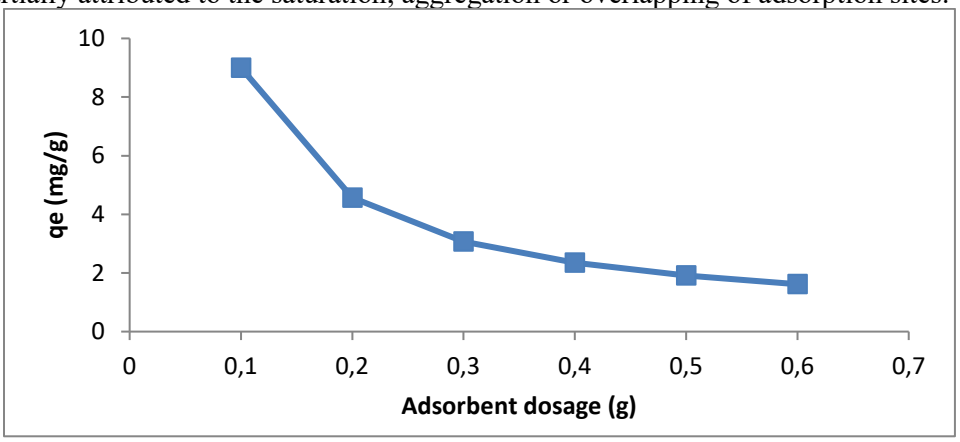

Fig. 7: Variation of q_e with Adsorbent Dosage

e. Impact of Initial Concentration

There is an important role for the initial concentration of the dye in adsorption process as a particular mass of adsorbent can only adsorb specific amount of a solute. The concentration of MO was varied at the range of 20 – 500 mg/L and adsorption capacity was found to increase from 9.61 – 247.22 mg/g as illustrated in Fig. 8. This obviously proves the dependency of adsorption process to the initial concentration of the dye. Increase in initial dye improve the interaction between the dye and adsorbent providing essential driving force to overcome the mass transfer resistance of the dye [23].

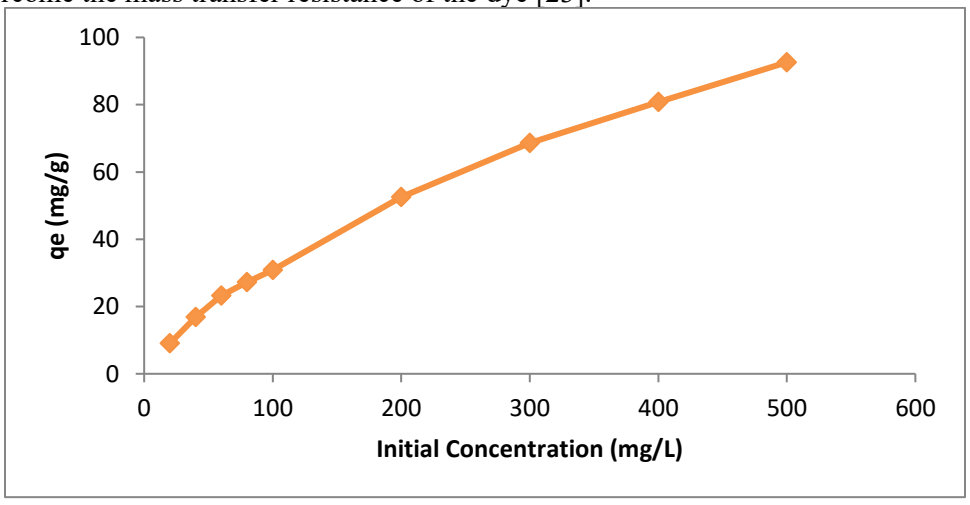

Fig. 8: Variation of q_e with Initial Concentration

f. Impact of Particle Size

The surface area usable for adsorption is largely affected by adsorbent particle size. greater number of adsorption sites and adsorption power resulted from the large surface area of adsorbent. The resulted presented in Fig. 9 shows the effect of adsorbent particle size on the sorption of MO onto GBAC. As the adsorbent particle size increases the amount of extracted dye decreases slowly. The highest adsorption capacity of 9.51 mg/g was obtained at 75 µm which decreased to 4.41 mg/g at 900 µm. The decrease in adsorption capacity with increase in particle size could be due to the less surface area thus lower the number of active adsorption sites.

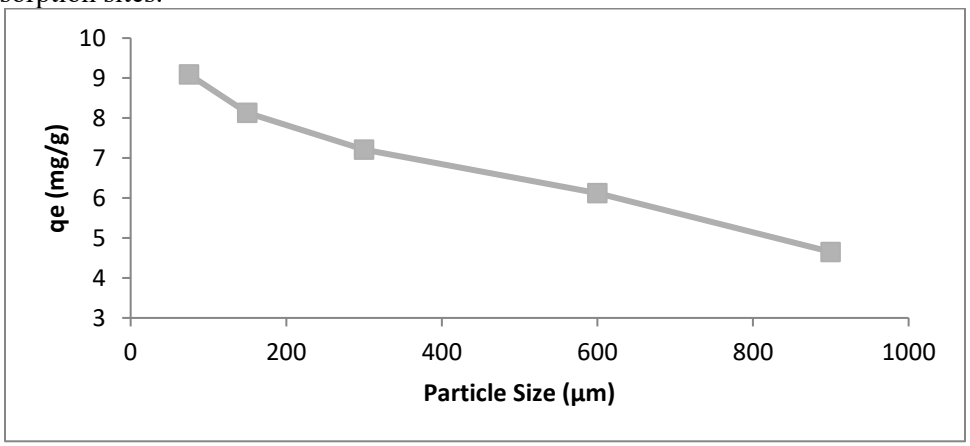

Fig. 9: Variation of q_e with Particle Size

g. Impact of Solution pH

Methyl orange dye is anionic dye that carries negative ion in aqueous solution. As ionic specie its adsorption can basically be controlled by the adsorbent surface charge which is influence by the pH solution. The pH of the solution was studied at the range of 2 - 12 adjusted by the dilute solution of NaOH and HCl. The variation of adsorption capacity versus solution pH is illustrated in Fig. 10 and the adsorption capacity decreases with increase in the solution pH. This indicates that the acidic pH condition preferred the adsorption anionic dye. The amount of MO adsorbed decreases from 9.82 mg/g at pH = 2 to 8.36 mg/g at pH = 12. The high MO adsorption capacity at lower pH is due to positive charge surface of the adsorbents, this can be explain in a better way by using pH at point of zero charge (pHpzc). The pHpzc value of GBAC was 5.9, this implies that at pH less than this value, the adsorbent surfaces get a net positive which enhances the adsorption of anionic dye such as methyl orange due to electrostatic attraction between the negative charge ion of the dye and positively charge surface of the adsorbent.

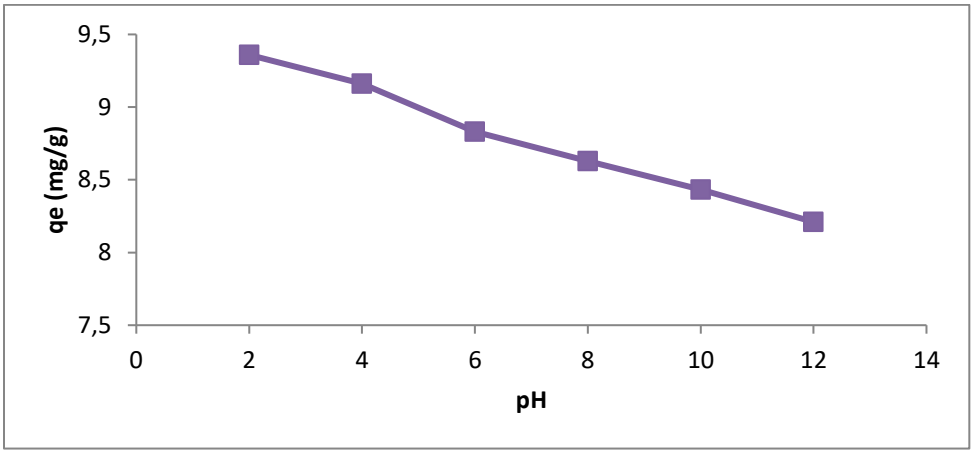

Fig. 10: Variation of q_e with pH

h. Impact of Temperature

The influence of temperature on methyl orange adsorption onto GBAC was studied at temperature ranges from 303 – 323 K. It can be seen that the variation of adsorption capacity decreases with increase in temperature as illustrated in Fig. 11. The adsorption capacity obtained at 303 and 323 K are 9.72 and 9.00 mg/g. This indicates that lower temperature favored the adsorption process which is a characteristic of exothermic process. An increase in temperature usually increased kinetic energy of the solute which enhances the rate for the diffusion of adsorbate molecules inside the adsorbent pores.

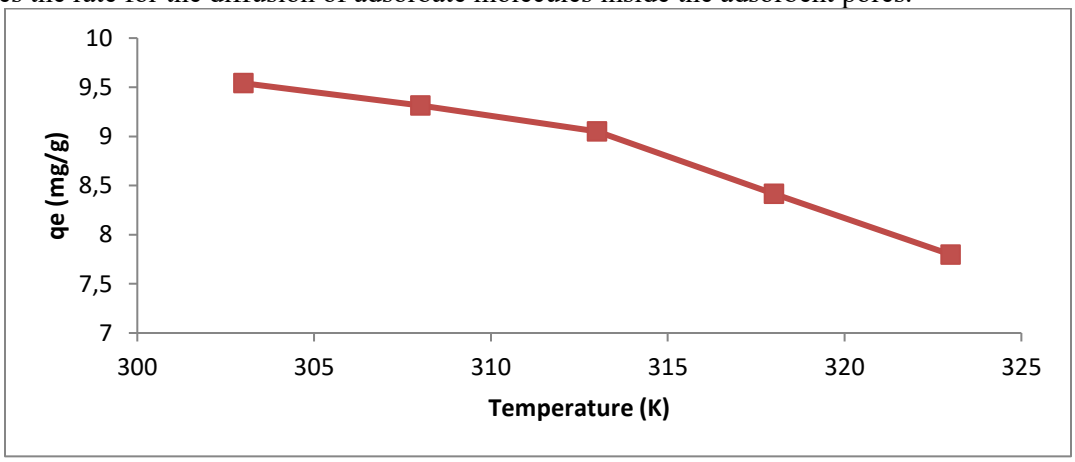

Fig. 11: Variation of q_e with Temperature

i. Thermodynamic Studies

Thermodynamic behavior of methyl orange adsorption onto GBAC was investigated and parameters such as Gibbs free energy change of adsorption (ΔG), enthalpy change (ΔH) and entropy change (ΔS) were evaluated using equation 5-7.

$$\Delta G = \Delta H - T\Delta S \quad (5)$$

$$K_c = \frac{C_{ads}}{C_e} \quad (6)$$

$$ln\ K_c = \frac{\Delta S}{R} - \frac{\Delta H}{RT} \quad (7)$$

Where C_{ads} and C_e are the concentration (mg/L) of the dye in adsorbed and liquid phase T is the temperature (K) and R is Gas constant with values 8.314 J/molK. The values ΔS and ΔH was estimated from the slope and intercept of plot of lnKc against inverse of T.

The evaluated values of thermodynamic parameters were presented in Table 2. The negative values of ΔG confirmed the adsorption of MO onto GBAC is feasible and spontaneous process. Decreases in negative values of ΔG with increasing temperature indicate that the adsorption is favored at lower temperature. However, the values of ΔG are less than -20 kJ/mol which implies that the adsorption is dominated by physical forces [24]. The negative values of ΔH and ΔS indicate the exothermic nature of the adsorption process and decrease in disorder of the adsorbate molecules onto the adsorbent.

j. Adsorption Kinetics

To further understand the mechanism of MO adsorption onto GBAC, kinetic studies of the sorption processes was conducted. The generated experimental data were tested by pseudo-first order and pseudo second order kinetic model. The best fitting model was chosen based on closeness of the obtained experimental adsorption capacity (q_{exp}) and calculated adsorption capacity (q_{cal}) values together with linear correlation coefficient (R^2) values. The experimental data were tested by pseudo first and second order kinetic models. The linear form of these models are given in equation 8 and 9

Pseudo-first order kinetic model; $\ln (q_e - q_t) = \ln q_e - k_1 t$ 8

Pseudo-second order kinetic model $\frac{t}{q_t} = \frac{1}{k_2 q_e^2} + \frac{t}{q_e}$ 9

Where q_e and q_t are the quantity (mg/g) of dye adsorbed at equilibrium and at time t (min) and k_1 and k_2 are the rates of adsorption constant for pseudo-first and second order.

The kinetic parameters obtained from the plot of pseudo-first-order and pseudo-second order models are illustrated in Table 3. It can be seen that the data fitted with pseudo-second-order model ($R^2 = 0.9994$). Furthermore, the theoretical adsorption capacity ($q_{e,\,cal} = 9.26$ mg/g) of this model is in agreement with the adsorption capacity ($q_{e,\,exp} = 9.00$ m/g) of the experimental value which confirmed the fitness of the model base on this comparison.

Table 3: Kinetic Parameters

Kinetic Model	Parameters	MO
Pseudo-first order	k_1(min^{-1})	0.06
	$q_{e\,exp}$ (mg/g)	9.00
	$q_{e\,cal}$ (mg/g)	4.83
	R^2	0.9350
Pseudo-second order	K_2 (g/ mg min)	0.03
	$q_{e\,exp}$ (mg/g)	9.00
	$q_{e\,cal}$ (mg/g)	9.26
	R^2	0.9994

l. Isotherm studies

Study of isotherm models gives highlight about the solutes molecules distribution between the liquid and solid phase at equilibrium. Experimental data was tested by four different common models i.e Freundlich, Langmuir, Temkin and D-R adsorption isotherm and the values are presented on Table 4. Examination of these isotherm parameters base on linear regression coefficient (R^2) of each model hinted that Freundlich isotherm emerged the best fitting model for the MO adsorption onto GBAC. The suitability of the Freundlich isotherm acquainted the multilayer coverage of the dye on the heterogeneous adsorbent surface [25]. The adsorption intensity n value was found to be greater than 1 which show the physical nature of the adsorption process.

Table 4: Adsorption Isotherm Parameters

Isotherm Model	Parameters	MO
Langmuir	q_m (mg/g)	48.54
	K_L (L/mg)	0.11
	R_L	0.31
	R^2	0.9274
Freundlich	K_F (mg/g)(L/mg)$^{1/n}$	6.83
	n	2.22
	1/n	0.45
	R^2	0.9935
Temkin	K_T (L/mg)	0.39
	b_T (kJ/mol)	16.35
	R^2	0.8928
D-R	q_m (mg/g)	43.60
	β (mol^2/J^2	1×10^{-6}
	E (kJ/mol)	0.71
	R^2	0.5043

m. Regeneration and Reusability Studies

The result of four different regenerate obtained from desorption studies are presented in Fig. 12. Sodium hydroxide with highest desorption efficiency of 70.02 % was considered as the best desorbing agent while distilled water was found to have the least desorbing ability with 8.23 % efficiency among the tested regenerate. The availability of $(OH)^-$ in basic medium make desorption of MO more favorable and therefore chosen to be the best desorbing medium.

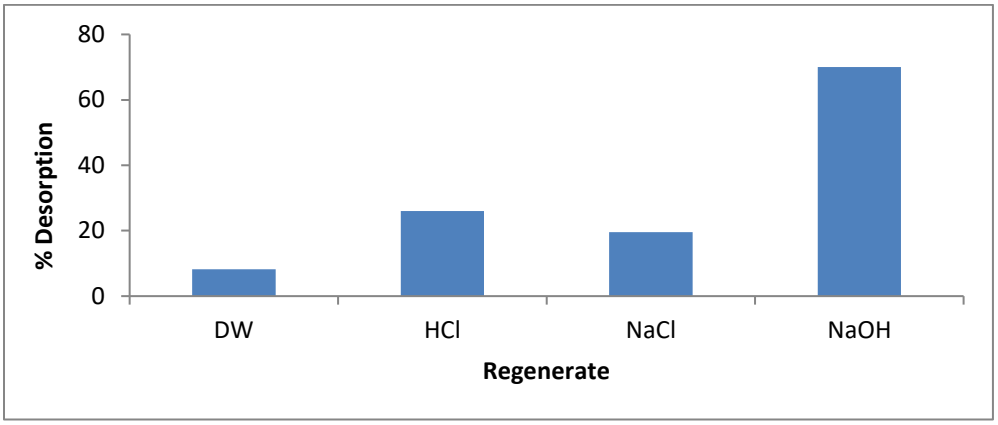

Fig. 12: Selection of Desorbing Medium

Fig. 13 presented the effect of contact time on desorbing medium and it shows the increase in desorption efficiency with increase in contact time until it reached the equilibrium time at 30 minute where 70.01 % was observed. Fig. 14 also presented the initial concentration effect on the desorbing medium and it was observed that increase in sodium hydroxide concentration increased desorption of MO from 48.21 % at 0.1M to 70.02 % at 0.5 M sodium hydroxide concentration.

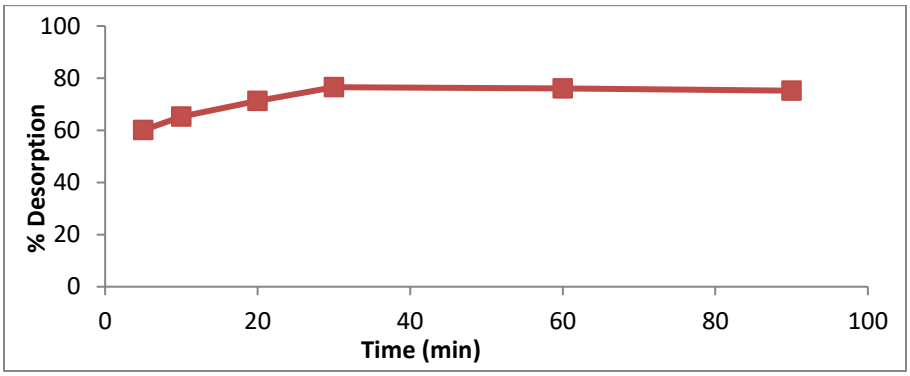

Fig. 13: Effect of Contact Time on Desorption

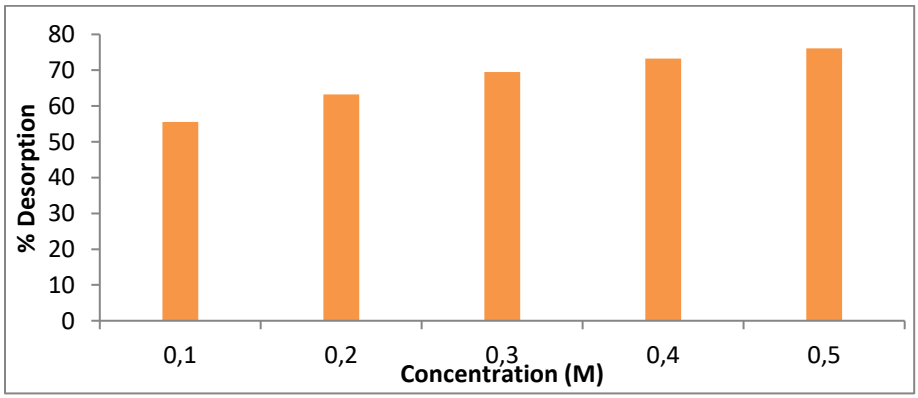

Fig. 14: Effect of Concentration of Desorbing Medium

The spent adsorbent was reused after the adsorption up to five numbers of different cycles. Fig. 15 illustrated the decrease in the efficiency of adsorption from 90.01 % in the first cycle to 63.42 % in the fifth cycle. The decrease in adsorption efficiency after each number of cycles is due to the decrease of active site after every adsorption cycle. This proves that GBAC can be used successfully for MO removal after different number of cycles.

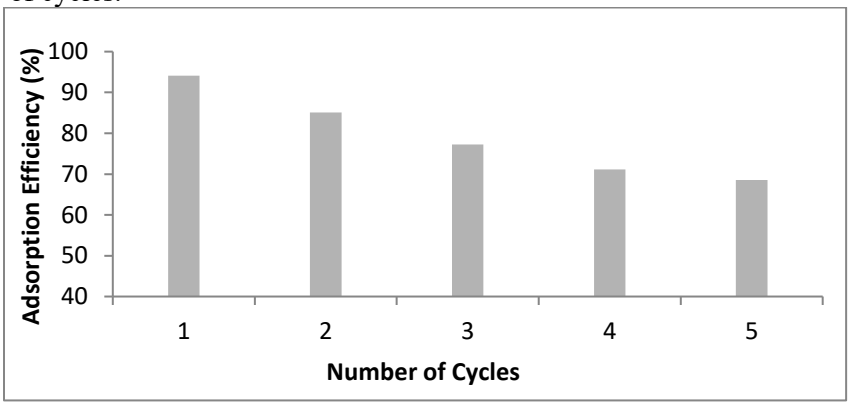

Fig. 15: Efficiency of regenerated adsorbent after five cycles

4. Conclusion

From the present research it can be concluded that sweet detar seed shell activated carbon was an effective and potential adsorbent for the removal of methyl orange dye from aqueous solution. The successful adsorption process was confirmed by FT-IR and SEM adsorbent characterization before and after the adsorption process. The studied experimental parameters such as contact time, adsorbent dosage, particle size, initial dye concentration, pH and temperature were found to influence the adsorption process. MO dye adsorption onto GBAC followed pseudo-second order model kinetically and accord with Freundlich adsorption isotherm model. Thermodynamic studies revealed the process to be exothermic, spontaneous and decreased in randomness of adsorption process on the adsorbent-liquid surface. Sodium hydroxide emerged as the best desorbing agent and the adsorbent could be reused up to five consecutive cycles.

Conflicts of Interest

The authors declare that they have no competing interests

References

1. Wong, J. K. H., Tan, H. K., Lau, S. Y., Yap, P. S. Danquah, M. K. *J. Environ. Chem. Eng.,* 7(2019) 103261.
2. Benkhaya, S., Mrabet, S. and El-Harfi, A. *Inorg. Chem. Commun.,* 115(2020) 107891.
3. Chen, J., Xiong, Y., Duan, M., Li, X., Li, J., Fang, S., Qin, S. and Zhang, R. *Langmuir*. 36(2020)520–533.
4. Znad, H., Abbas, K., Hena, S. and Awual, M. R. *J. Environ. Chem. Eng.,* 6 (2018) 218–227.

5. Sahoo, C. and Gupta, A. K. J. Environ. Sci. Health, Part A: Toxic/Hazard. Subst. Environ. Eng., 50(2015) 1333–1341.
6. Hynes, N. R. J., Kumar, J. S., Kamyab, H., Sujana, J. A. J., Al-Khashman, O. A., Kuslu, Y., Ene, A. and Kumar, B. S. *J. Cleaner Prod.,* 272(2020)122636.
7. Deering, K., Spiegel, E., Quaisser, C., Nowak, D., Rakete, S., Garı, M. and Bose, S. and Reilly, O. *Environ. Res.,* 184(2020) 109271.
8. Lellis, B., Favaro, C. Z., Pamphile, J. A. and Polonio, J. C. Biotechnol. *Res. Innov.,* 3(2019) 275–290.
9. Meerbergen, K., Crauwels, S., Willems, K. A., Dewil, R., Van, J., Appels, I. L., Lievens, B. and J. Biosci. *Bioeng.,* 124: 668–673.
10. Gupta, B., Priya, T. and Kumar , B. M. *Environ. Eng. Res.,* 26(2020) 200234.
11. Shaban, M., Abukhadra, M. R., Hamd, A., Amin, R. R. and Abdel, A. K. *J. Environ. Manage.,* 204 (2017) 189–199.
12. Samsami, S., Mohamadi, M., Sarrafzadeh, M. H., Rene, E. R. and Firoozbahr, M. *Process Saf. Environ. Prot.,* 143(2020) 138–163.
13. Yadav, M. K., Saidulu, D., Gupta, A. K., Ghosal, P. S. and Mukherjee, A. *J. Environ. Chem. Eng.,* 9(2021) 105203.
14. Jadhav, S. K. and Thorat, S. R. *Biosciences biotechnology research.* 19(1) (2022)141-151.
15. Ibrahim, M.B. and Sani, S. Neem (*azadirachta indica*). *Journal of Geosciences and Environmental protection,* 3(2015)1-9. https://doi.org/10.4236/gep.2015.32001
16. Husaini, M., Usman, B., Ibrahim M. A. and Ibrahim, M. B. *Res. J. Chem. Environ*., 24(2) (2020) 99-106.
17. Ayuba, A. M., Hamza, U., Shurahabil, I. B., and Abdulmumini, H. *UMYU Scientifica*. 1(1) (2022) 91 – 102
18. Ibrahim, M.B., Sulaiman, M.S., Sani, S. Assessment of adsorption properties of neem leaves waste for the removal of congo red and methylene orange. 3rdn international conference on biological, chemical and environmental sciences (BCES-2015) September 21-22, 2015 Kuala Lampur, Malaysia (2015).
19. Ayuba, M.A., Bridget, I *Arabian Journal of Chemical Research.* 8(1) (2021) 114-132.
20. Shakoor S, Nasar A *Cellulose* 7(2020) 30–38.
21. Giwa AA, Oladipo MA, Abdulsalam KA. *ournal of Chemical and Pharmaceutical Research*.;7(2) (2015)454-475.
22. Wanyonyi WC, Onyari JM, Shiundu PM. *Energy Procedia*.;50 (2014)862-869.
23. Enenebeaku, K.C., Okorocha, J.N., Enenebeaku, E.U., Okolie, I.J., Anukum, B. *IOSR Journal of applied Chemistry*, e-ISSN: 2278-5736, 9 (9) (2016) 28-38. https://doi.org/10.9790/5736-0909012838

24. Laabd M, Chafai H, Essekri A, Elamine M, Al-Muhtaseb SA, Lakhmiri R, Albourine A. *Sustainable materials and technologies*. 12(2017)35-43.
25. Usman, B., Bello, A.U. and Adeleke, R. *Arabian Journal of Chemical and Environmental Research. 9(1)* (2022) *86-9.*